



Article

Experimental Research on the Impact Resistance Mechanical Properties and Damage Mechanism of Rubberized Concrete under Freeze–Thaw Cycling

Xiaowen Huang ^{1,2,3,*}, Tengsheng Yue ^{1,*}, Jun Zhang ¹ and Jinsong Zhang ^{1,2,3}

¹ Anhui Province Key Laboratory of Green Building and Assembly Construction, Anhui Institute of Building Research & Design, Heifei 230031, China; jun_zhang121@163.com (J.Z.); zjswwhy890723@126.com (J.Z.)

² National Key Laboratory of Fine Coal Exploration and Intelligent Development, China University of Mining and Technology, Xuzhou 221116, China

³ School of Civil Engineering and Architecture, Anhui University of Science and Technology, Huainan 232001, China

* Correspondence: hxw2022147@163.com (X.H.); ytfaylinn@sina.cn (T.Y.)

Featured Application: The study of the freeze–thaw cycling and impact resistance properties of rubberized concrete materials can provide a better understanding and mastery of the durability performance of rubberized concrete materials. It holds significant theoretical and practical value for actual engineering projects in cold regions.

Abstract: To improve the long-term performance of concrete engineering in high-altitude areas, waste tire rubber was added to a concrete mix, and freeze–thaw and impact tests were conducted. The effects of waste tire rubber with different particle sizes (10, 20, 30 mesh) and freeze–thaw cycles (0, 25, 50, 75, 100, 125) on the dynamic mechanical properties of concrete materials were studied. The stress–strain curves, peak stress, and fracture morphology of the specimens were analyzed. The microstructure changes of the specimens were also analyzed using scanning electron microscopy (SEM). The results showed the following: (1) Both macroscopic and microscopic analysis results showed that the internal damage of rubber concrete specimens was smaller after freeze–thawing, and the integrity was better after impact, maintaining a loose but not scattered state. The addition of waste tire rubber significantly improved the material’s impact resistance to a certain extent. (2) As the impact pressure increased, the strain rate of the specimens increased linearly, and the dynamic peak stress was linearly positively correlated with the strain rate. (3) After 125 freeze–thaw cycles, the peak stress of the specimens with 30-mesh added rubber decreased significantly less than that of ordinary concrete under 0.3, 0.45, and 0.6 MPa impact pressure. The dynamic peak stress was higher than that of specimens with 10-mesh and 20-mesh added rubber, and the addition of 30-mesh rubber significantly improved the frost resistance and impact resistance of concrete materials. This study can provide new ideas for the engineering application of rubber concrete.



Citation: Huang, X.; Yue, T.; Zhang, J.; Zhang, J. Experimental Research on the Impact Resistance Mechanical Properties and Damage Mechanism of Rubberized Concrete under Freeze–Thaw Cycling. *J. Compos. Sci.* **2024**, *8*, 87. <https://doi.org/10.3390/jcs8030087>

Received: 14 November 2023

Revised: 25 December 2023

Accepted: 2 January 2024

Published: 27 February 2024

Keywords: rubber concrete; freeze–thaw cycle; dynamic impact; frost resistance



Copyright: © 2024 by the authors. Licensee MDPI, Basel, Switzerland. This article is an open access article distributed under the terms and conditions of the Creative Commons Attribution (CC BY) license (<https://creativecommons.org/licenses/by/4.0/>).

1. Introduction

Since the 1990s, China has begun to vigorously develop road infrastructure construction and has become the country with the largest total mileage of highways in the world. A traditional highway is generally poured with ordinary concrete. Although it has high strength and good bearing capacity, its ductility, bending resistance, and deformation resistance are small, and the joints are prone to damage. It is difficult to repair, and the applicable conditions are not universal. In addition, there is asphalt concrete pavement; asphalt concrete pavement is more comfortable and elastic than cement concrete pavement, but its durability and bearing capacity are poor. China has a high difference in altitude

between the east and west and a large difference in latitude between the north and south. Some areas at high altitudes have snow-frozen soil for most of the year. The lowest outdoor temperature in northern winter can reach minus 40 degrees, especially in the northeast and northern Inner Mongolia. The climate is cold and dry, and there is much snowfall, which makes the road freeze and affects traffic operation. We usually take measures to thaw the road to reduce the impact of traffic on people's travel. Due to the climate and these thawing measures, the road is constantly undergoing a freeze–thaw cycle, destroying the internal structure of the concrete and causing damage to the road. This affects the service performance and driving safety of the highway. The highway requires a lot of manpower and material resources to repair, and more seriously, it even needs to be demolished and rebuilt. China spends a lot of money on highway maintenance and repair every year.

It is found that the incorporation of rubber into concrete can effectively improve some properties of concrete, and road laying can prolong its service life and crack resistance [1–3]. Wei Li et al. [4] studied the fracture properties of rubber concrete with different contents and found that rubber could improve the interface effect between rubber and the cement base and improve the crack resistance of concrete. At the same time, some other scholars have also found that the addition of rubber improves the toughness and crack resistance of concrete [5–7]. However, it was found that the incorporation of rubber significantly reduced the compressive strength of concrete [8–10]. Many scholars have found that rubber can improve the durability of concrete [11–15]. Habib Akbarzadeh Bengar et al. [16] studied the chloride resistance of concrete by adding rubber with different particle sizes and different contents. The results showed that the incorporation of rubber could significantly improve the chloride resistance of concrete. When the rubber particle size was 3–6 mm and the content was 5%, the corrosion resistance was the best. Rubber can significantly improve the impact resistance of concrete [17–19]. Abbas Safeer et al. [20] conducted impact resistance tests on rubber concrete with different particle sizes and different contents. The results show that selecting the best rubber replacement rate and rubber size can significantly improve the impact resistance of concrete. At the same time, rubber can improve the frost resistance of concrete [21]. In addition, the anti-aging and sound insulation [22,23] effects of rubber concrete are better than those of ordinary concrete, and the incorporation of rubber into concrete can effectively alleviate the thorny problem of waste tire rubber [24–26].

At present, there are a lot of studies on the toughness, durability, and static mechanical properties of rubber concrete under complex conditions, but there are relatively few studies on dynamic mechanical properties. In order to make rubber concrete more common and practical in the future construction industry, based on the research results of other scholars [20,27,28], taking 20% sand quality as the rubber quality, we added 10-mesh, 20-mesh, and 30-mesh rubber made of waste tires to concrete. The static compressive and dynamic impact properties of rubber concrete with different particle sizes under freeze–thaw cycles were studied.

2. Materials and Methods

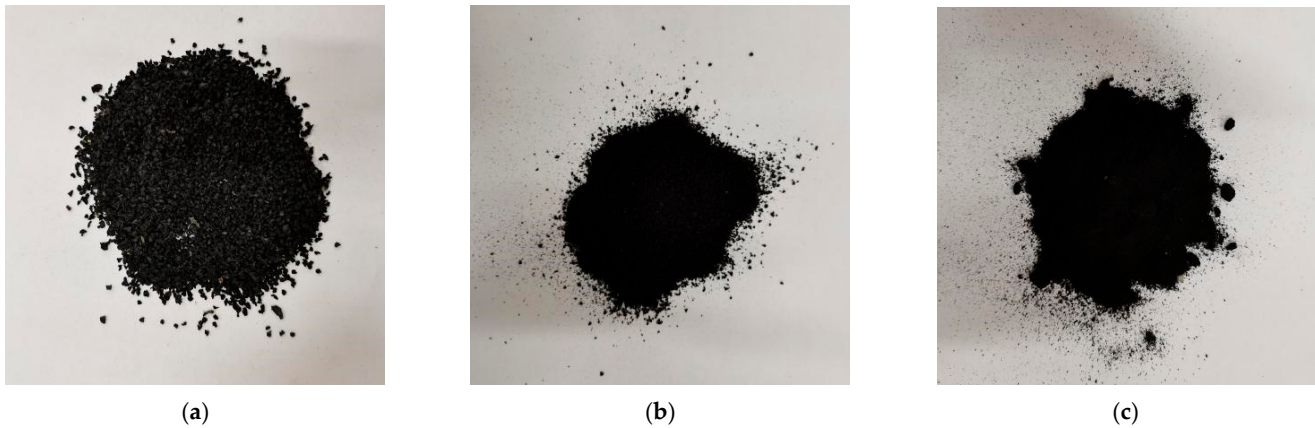
2.1. Raw Material

The test cement, P.O 42.5 ordinary Portland cement, was produced by the Bagongshan Cement Plant in Huainan City. The sand used was natural river sand; its fineness modulus was 2.80, apparent density was 2520 kg/m³, and bulk density was 1640 kg/m³. The stone used was natural gravel; the particle size was 5–16 mm, the apparent density was 2625 kg/m³, and the bulk density was 1665 kg/m³. The water-reducing agent was PCA polycarboxylate superplasticizer. Water was ordinary tap water. Waste tire rubber was 10-mesh, 20-mesh, and 30-mesh rubber produced by Dujiangyan Huayi Rubber Co, Ltd. The apparent density was 750 kg/m³, and the specific size of the rubber is shown in Table 1 and Figure 1.

Table 1. Rubber size.

Rubber Standard Mesh Number	10 Mesh	20 Mesh	30 Mesh
Average particle size	2.00 mm	0.850 mm	0.600 mm

Note: The number of holes is the number of holes per square inch. The larger the mesh number, the smaller the aperture.

**Figure 1.** Rubber: (a) 10 mesh; (b) 20 mesh; (c) 30 mesh.

2.2. Specimen Preparation

In this experiment, the mix ratio design was mainly based on the concrete design specifications. The concrete mix ratio of C40 was used to calculate the amount of coarse aggregate, fine aggregate, cement, water, and so on. With 20% fine aggregate mass as the amount of waste tire rubber, 10-mesh, 20-mesh, and 30-mesh waste tire rubber were directly mixed into C40 concrete. Group A was not mixed with waste tire rubber, group B was mixed with 20% 10-mesh waste tire rubber, group C was mixed with 20% 20-mesh waste tire rubber, and group D was mixed with 20% 30-mesh waste tire rubber. Since waste tire rubber is a hydrophobic material, in principle, the amount of water and water-reducing agent does not need to be changed. The detailed mix ratio is shown in Table 2.

Table 2. Test mix ratio.

Group Number	Fine Aggregate kg/m ³	Coarse Aggregate kg/m ³	Cement kg/m ³	Waste Tire Rubber		Water kg/m ³	Water-Reducing Admixture kg/m ³
				Mesh Number	Dosage kg/m ³		
A	581.43	1356.67	329.60		0	132.30	3.30
B	581.43	1356.67	329.60	10 mesh	58.14	132.30	3.30
C	581.43	1356.67	329.60	20 mesh	58.14	132.30	3.30
D	581.43	1356.67	329.60	30 mesh	58.14	132.30	3.30

Experimental steps of quick freezing method:

- (1) The prepared concrete test block was put into the saturated solution curing pool for 24 days and then soaked in $(20 \pm 2) ^\circ\text{C}$ water for 4 days. The water needed to pass through the top of the test block. After the test block was cured for 28 days, the freeze–thaw cycle test could be started [29,30].
- (2) Each freeze–thaw cycle time was 4 h, with rapid freezing for 2.5 h and then rapid melting for 1.5 h. The temperature of the low-temperature freezing equipment was set to $-20 ^\circ\text{C}$. The test block containing saturated water was frozen in the low-temperature freezing equipment, and the melting was carried out in the clear water. A constant-temperature heating rod was added to the clear water to accelerate the melting and thawing speed of the test block.

- (3) Every 25 freeze–thaw cycles were a sequence. After each freeze–thaw sequence, 3 compressive test blocks and 9 impact test blocks were taken out from each group for mechanical testing. After each freeze–thaw sequence, the scum on the surface of the test block was washed with water, and the surface moisture was dried with a wet towel to measure the quality change.

2.3. Test Equipment and Scheme

The SHPB (Split–Hopkinson pressure bar) test device is mainly composed of three parts: a compression bar system including an impact bar, an incident bar, a transmission bar, and an absorption bar; a measurement system; and a data acquisition and processing system. Figure 2 is a schematic diagram of the SHPB device. This instrument is produced by Hunan Central South University.

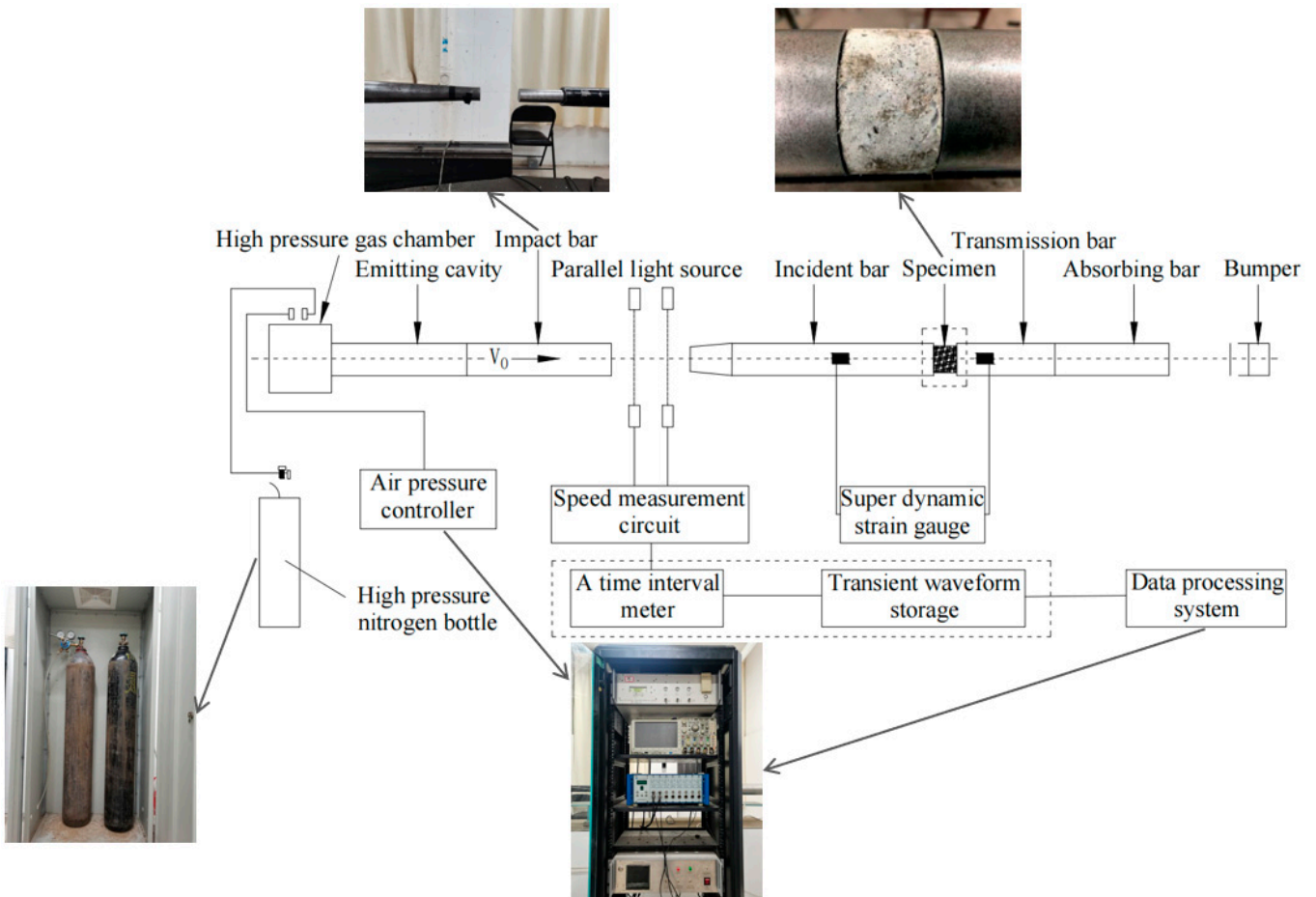


Figure 2. Schematic diagram of SHPB device.

The bar system of the SHPB test device was a 74 mm steel bar. The specimen was placed between the incident bar and the transmission bar. The air pressure generated by the nitrogen bottle caused the impact bar to eject the transmitting cavity at an initial velocity V and impact the incident bar. The incident wave was transmitted to the specimen along the bar, so that the specimen was subjected to a dynamic load. Before the test, strain gauges were pasted on the incident bar and the transmission bar. The position of the strain gauge was controlled so as not to be too close to the specimen, and the surface was pasted with insulating tape. On the one hand, the tape was used to protect the strain gauge, on the other hand, it was used to avoid contact between the strain gauge and the wire during the impact process causing data errors. The incident wave, reflected wave, and transmitted

wave generated during the impact process were transmitted by the strain gauge to the data acquisition and processing system.

The SHPB test was based on the one-dimensional elastic wave theory and the assumption that the stress and strain are uniformly distributed in the specimen [31]. The following can be concluded:

Average stress:

$$\sigma_s(t) = \frac{EA}{A_s} \varepsilon_t = \frac{EA}{A_s} (\varepsilon_i + \varepsilon_r)$$

E —elastic modulus of compression bar;

A —the cross-sectional area of the strut;

A_s —cross-sectional area of specimen;

ε_t —transmitted wave;

ε_i —incident wave;

ε_r —reflected wave.

Average strain:

$$\varepsilon_s(t) = \frac{2C_0}{l_0} \int_0^t (\varepsilon_i - \varepsilon_t) dt = -\frac{2C_0}{l_0} \int_0^t \varepsilon_r dt$$

C_0 —longitudinal wave velocity;

l_0 —initial length of specimen.

Average strain rate:

$$\dot{\varepsilon}_s(t) = \frac{2C_0}{l_0} (\varepsilon_i - \varepsilon_t) = -\frac{2C_0}{l_0} \varepsilon_r$$

In this experiment, a Hopkinson bar with a diameter of 74 mm was used to conduct dynamic tests on ordinary concrete and rubberized concrete with different particle sizes after different freeze–thaw cycles. The experimental situation is shown in Figure 3. The specimens were subjected to impact tests with three different pressures of 0.3 MPa, 0.45 MPa, and 0.6 MPa after undergoing different numbers of freeze–thaw cycles. Three specimens were selected for each test condition.



Figure 3. The 74 mm diameter SHPB device physical map.

3. Dynamic Impact Test Results and Analysis

3.1. Microstructure Analysis of Freeze–Thaw Cycle

The SEM images of ordinary concrete and 30-mesh rubber concrete after 0 and 125 freeze–thaw cycles are shown in Figure 4.

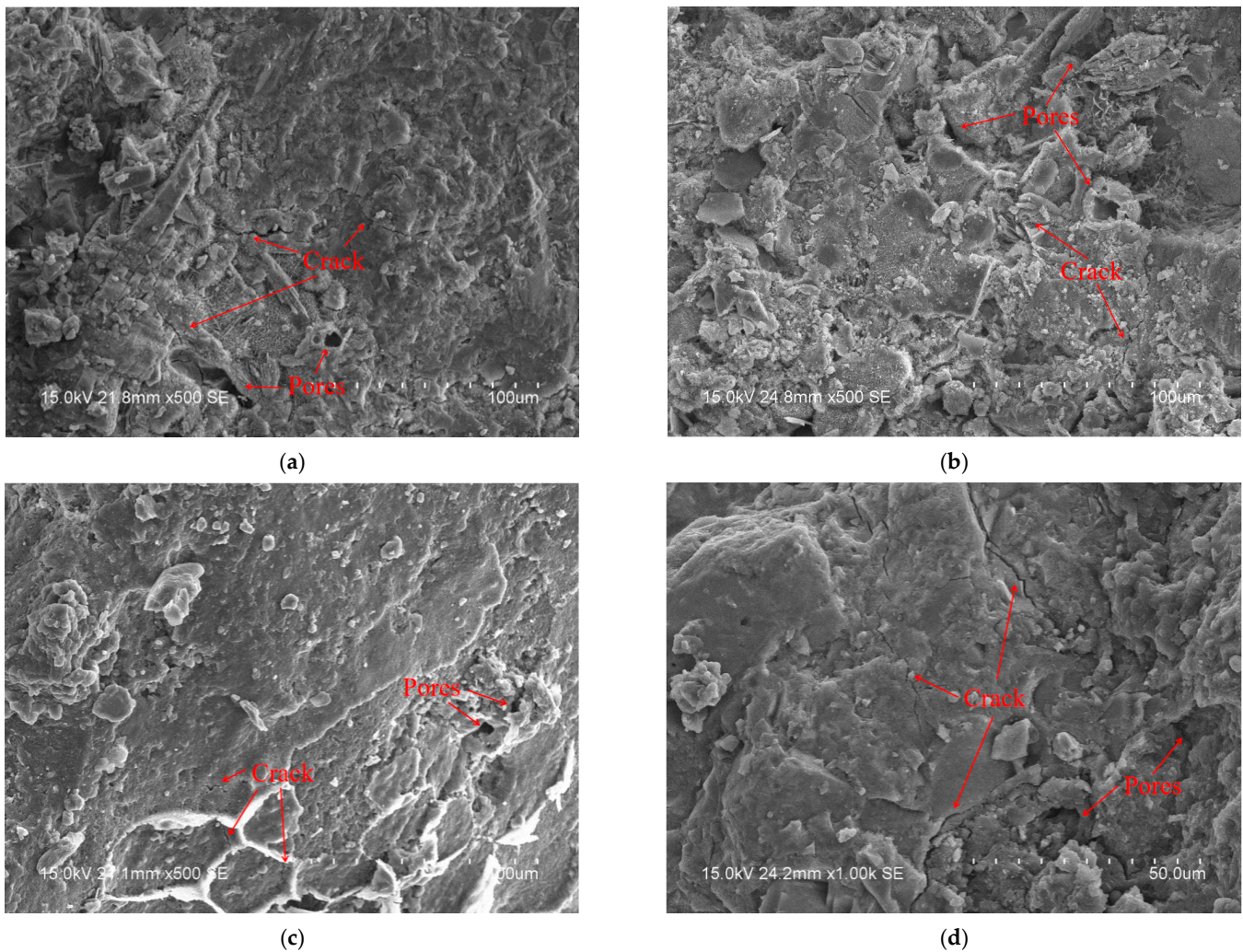


Figure 4. Microstructure SEM. (a) Concrete 0 freeze–thaw; (b) concrete 125 freeze–thaw; (c) 30-mesh rubber concrete 0 freeze–thaw; (d) 30-mesh rubber concrete 125 freeze–thaw.

As shown in Figure 4a,b, there are some holes and cracks in ordinary concrete without freeze–thaw cycles. After 125 freeze–thaw cycles, the holes increase, the cracks widen, and the concrete becomes loose. As shown in Figure 4c,d, there are some holes and cracks in rubber concrete without freezing and thawing. As the number of freezing and thawing cycles increases, the cracks expand, becoming wider and longer, and the holes also increase. However, compared with ordinary concrete, the pores are smaller and more when there is no freeze–thaw cycle, indicating that the incorporation of rubber introduces some bubbles in the concrete. After 125 freeze–thaw cycles, the pores of rubber concrete increase relatively little, the cracks increase more, and the holes are denser. The reason is that the incorporation of rubber introduces more small pores. When the concrete freezes, the internal pores relieve the water pressure and the volume increases occurring when the water freezes, which slows down the internal damage. However, when the pores increase and the damage occurs, the pores are more likely to merge and form cracks. Therefore, compared with ordinary concrete, the cracks increase more, but the internal damage is smaller, the integrity is better, and the concrete has stronger frost resistance. Further, due to the freezing and thawing cycle, the temperature decreases, and the water undergoes a phase change and turns into ice, forming an ice lens. With an increase in the number of freezing and thawing cycles, the ice lenses continue to grow larger and more numerous. When the cycle reaches 125 times, the internal ice lens content of the sample is higher, and the overall integrity of the sample is good.

3.2. Test Failure Mode

The fracture morphology of the specimens with 0 and 125 freeze–thaw cycles under different impact pressures is shown in Table 3.

Table 3. Dynamic impact experiment phenomenon of freeze–thaw cycle.

Group Number	0 freeze–thaw cycles	125 freeze–thaw cycles	0.3 MPa	0.45 MPa	0.6 MPa
A	0 freeze–thaw cycles				
	125 freeze–thaw cycles				
B	0 freeze–thaw cycles				
	125 freeze–thaw cycles				

Table 3. Cont.

Group Number	0.3 MPa	0.45 MPa	0.6 MPa	
C	0 freeze–thaw cycles			
	125 freeze–thaw cycles			
D	0 freeze–thaw cycles			
	125 freeze–thaw cycles			

It can be seen from the comparison that the rubber concrete has better integrity after impact, and there is no large breakage. Most of the specimens only have cracks or become loose between the materials after compression. The whole specimen is loose but not scattered, showing better integrity. Under the impact of 0.3 MPa pressure, the failure phenomenon of the specimens in groups B, C, and D is not obvious. Under the impact of 0.45 MPa air pressure, there are more cracks on the specimen, and part of the outer edge of the specimen falls off. Under the impact of 0.6 MPa pressure, the cracks on the specimen become more and deeper. As the number of freeze–thaw cycles increases, the specimen becomes loose after impact, or some small pieces peel off from the specimen, and the peeled part is a complete small piece. The overall integrity of rubber concrete specimens is good,

which is different from the fine particles formed by ordinary concrete after impact. On the whole, rubber concrete is not easy to crush after impact, and the integrity is better. By comparing the failure modes of concrete without the addition of concrete and rubber concrete with different particle sizes, it can be seen that the integrity of the specimen after impact is better when rubber concrete is added. Further comparison of the failure modes of rubber with different mesh sizes shows that the fracture of the specimen becomes more pronounced with the increase in rubber particles added. This is mainly due to the addition of rubber particles, which increases the contact surface between the concrete composition and rubber, making the specimen more prone to deformation and failure under impact.

Based on the research results of some scholars and the phenomenon of this experiment, the reasons for the above are analyzed [32,33]: in the process of the freeze–thaw cycle, the internal cracks of the specimen gradually increase with the increase in the number of freeze–thaw cycles, and the connection between the cracks makes the gap larger. After the impact, the specimen is more easily broken. Therefore, after 125 freeze–thaw cycles, the impact failure of the specimen is more obvious. The strain rate of ordinary concrete increases with the increase in impact pressure. The instantaneous damage of the impact does not easily occur at the weakest point, and the specimen is subjected to more small damage, which then penetrates into large cracks. The higher the strain rate is, the more small cracks and large cracks are formed. As a brittle material, concrete breaks after the cracks are generated, and the damage to concrete specimens is more crushing. After the rubber concrete is impacted, the rubber absorbs part of the energy and delays the action of the force inside the specimen. Therefore, the failure phenomenon is not obvious compared with ordinary concrete. Rubber as an elastic material increases the plasticity of concrete. After the concrete is impacted, the force first acts on the interface between rubber and cement mortar, then acts on the cement mortar around the rubber, and then acts on the interface between cement mortar and coarse aggregate. The incorporation of rubber makes the concrete have a certain toughness. Under the action of force, although the rubber concrete is damaged, it does not easily break directly, and only intricate cracks are generated. The ordinary concrete and rubber concrete after the test were hammered along the cracks, and it was found that the ordinary concrete was brittle and directly disconnected, and the disconnected surface was relatively flat. In rubber concrete, due to the incorporation of rubber, elastic rubber is connected with some aggregate, and aggregate, due to the connection of rubber, does not easily fracture directly. When subjected to impact, these weak joints are not directly broken, although they are damaged by force. The integrity is good, and the fracture surface is rough after the specimen is broken.

3.3. Stress–Strain Curve

A group of dynamic peak stresses closest to the average value was selected for result analysis. The test results obtained are shown in Table 4, and the stress–strain curves of the specimens after different freeze–thaw cycles are shown in Figure 5.

Table 4. Mechanical parameters under different impact pressures after different freeze–thaw cycles.

Impact Pressure (MPa)		0.3 MPa		0.45 MPa		0.6 MPa	
Number of Freeze–Thaw Cycles	Group Number	Strain Ratio (s ^{−1})	Dynamic Peak Stress (MPa)	Strain Ratio (s ^{−1})	Dynamic Peak Stress (MPa)	Strain Ratio (s ^{−1})	Dynamic Peak Stress (MPa)
0	A	79.66	54.59	97.99	62.80	135.19	71.39
25		77.51	51.54	102.18	58.22	135.29	67.19
50		84.14	46.54	101.59	52.75	129.84	62.54
75		87.89	40.09	109.39	45.15	128.99	55.66
100		87.67	33.67	106.10	38.64	132.55	43.47
125		88.88	25.31	104.41	29.78	133.65	34.02

Table 4. Cont.

Impact Pressure (MPa)	0.3 MPa		0.45 MPa		0.6 MPa			
	Number of Freeze–Thaw Cycles	Group Number	Strain Ratio (s ⁻¹)	Dynamic Peak Stress (MPa)	Strain Ratio (s ⁻¹)	Dynamic Peak Stress (MPa)	Strain Ratio (s ⁻¹)	Dynamic Peak Stress (MPa)
0.3	0	B	81.60	37.63	107.02	45.20	120.46	48.77
	25		85.82	35.28	106.70	41.48	135.74	44.97
	50		86.13	32.52	104.89	37.41	133.54	41.16
	75		89.15	29.78	115.31	33.44	137.84	37.57
	100		84.72	25.20	109.93	28.98	135.96	33.21
	125		88.11	21.00	114.41	24.15	131.36	28.35
0.45	0	C	93.60	39.51	113.76	45.69	130.23	51.31
	25		90.38	37.79	108.79	42.38	126.08	48.52
	50		86.17	34.82	117.11	39.46	135.61	45.69
	75		88.65	31.06	105.45	35.28	130.38	41.23
	100		79.16	27.09	106.69	31.00	135.66	37.57
	125		82.31	23.71	107.24	26.13	130.44	31.21
0.6	0	D	79.96	42.15	101.43	49.33	127.46	55.63
	25		83.40	40.22	108.28	46.20	132.80	52.91
	50		79.11	37.72	103.10	43.52	127.85	50.62
	75		77.03	33.21	93.95	39.69	124.44	47.04
	100		82.84	30.54	101.09	35.89	127.97	43.01
	125		96.45	26.72	106.92	30.54	136.41	38.56

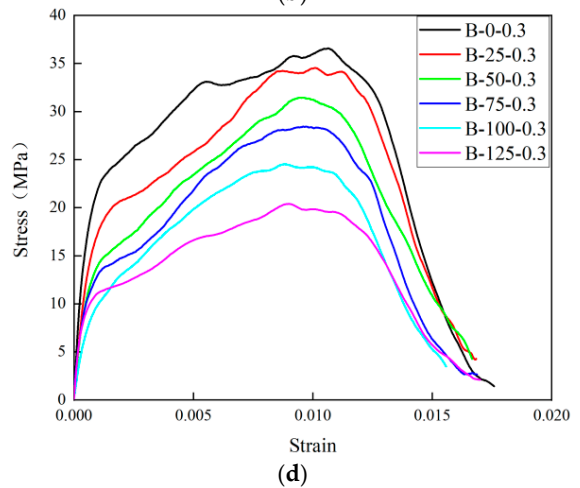
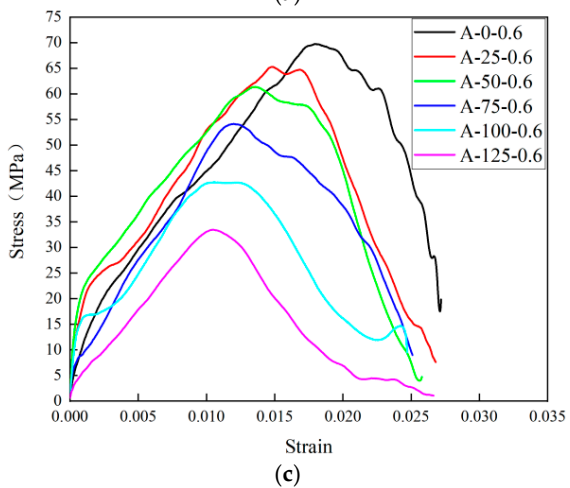
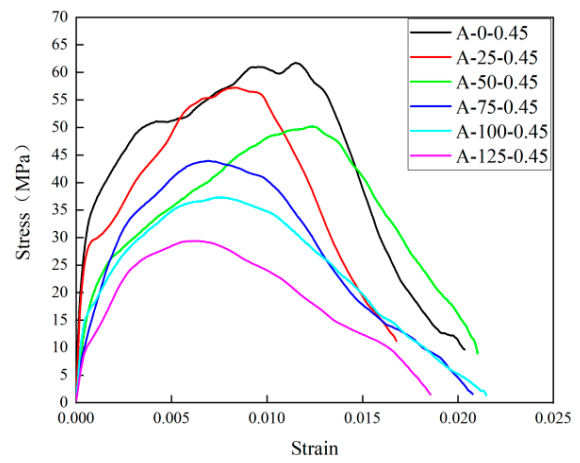
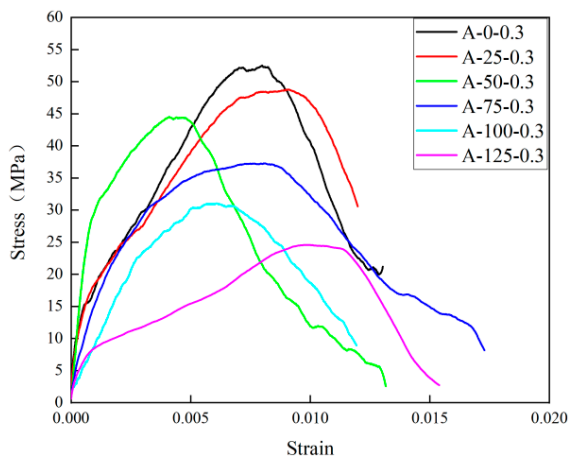


Figure 5. Cont.

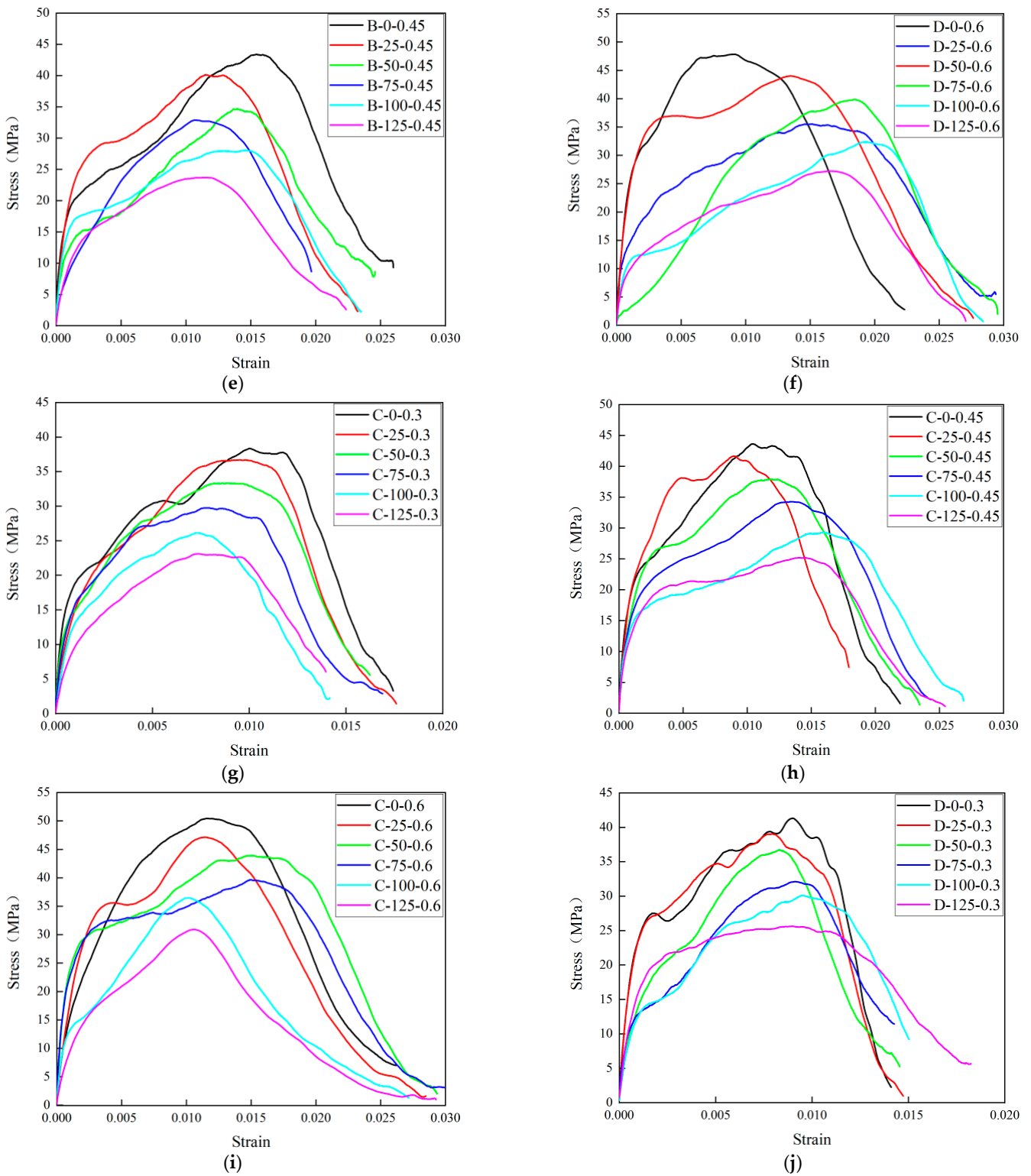


Figure 5. Cont.

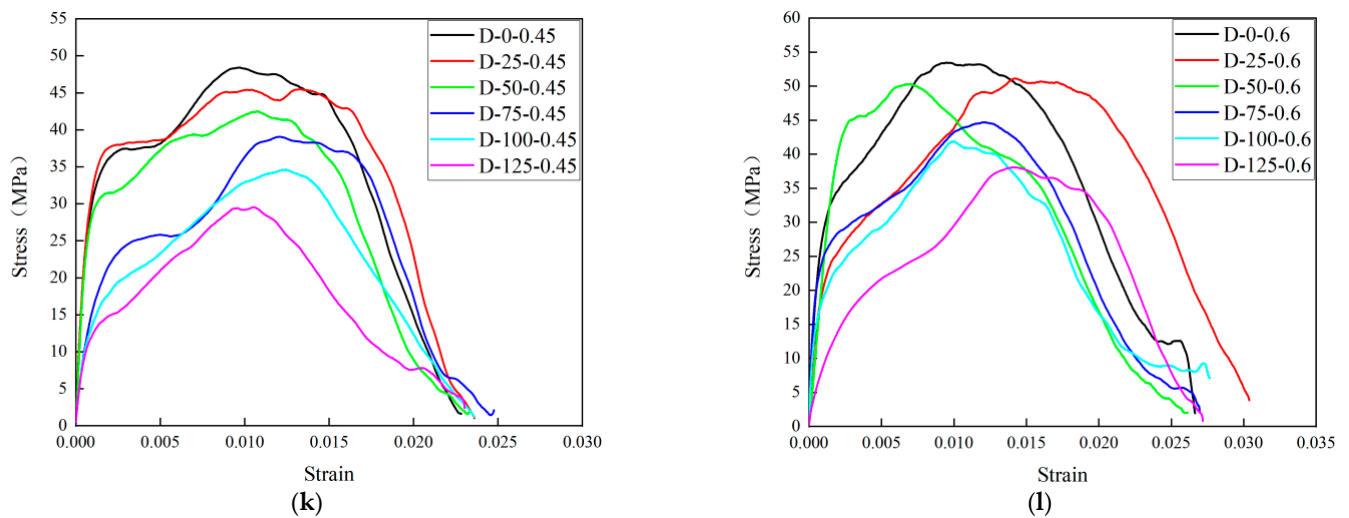


Figure 5. Stress–strain curves under different impact pressures after different freeze–thaw cycles. (a) Group A was impacted under 0.3 MPa pressure after freeze–thaw. (b) Group A was impacted under 0.45 MPa pressure after freeze–thaw. (c) Group A was impacted under 0.6 MPa pressure after freeze–thaw. (d) Group B was impacted under 0.3 MPa pressure after freeze–thaw. (e) Group B was impacted under 0.45 MPa pressure after freeze–thaw. (f) Group B was impacted under 0.6 MPa pressure after freeze–thaw. (g) Group C was impacted under 0.3 MPa pressure after freeze–thaw. (h) Group C was impacted under 0.45 MPa pressure after freeze–thaw. (i) Group C was impacted under 0.6 MPa pressure after freeze–thaw. (j) Group D was impacted under 0.3 MPa pressure after freeze–thaw. (k) Group D was impacted under 0.45 MPa pressure after freeze–thaw. (l) Group D was impacted under 0.6 MPa pressure after freeze–thaw.

In the same group of specimens, the strain rate of the specimen increases with the increase in the impact pressure. When the number of freeze–thaw cycles is the same, the peak stress of the specimen increases with the increase in the impact pressure; that is, the greater the impact pressure, the greater the peak stress of the specimen. Under the same impact pressure, the peak stress of the specimen decreases with the increase in the number of freeze–thaw cycles.

In different groups of specimens, when the impact pressure and the number of freeze–thaw cycles are the same, the peak stress of group A is higher than that of groups B, C, and D. With the increase in particle size, the peak stress of rubber concrete is generally lower. Therefore, the smaller the particle size of rubber, the smaller the impact on the peak stress of concrete. From 0 to 125 freeze–thaw cycles, the peak stress reduction ratio of groups B, C, and D was smaller than that of group A under the same air pressure. Compared with groups B, C, and D, the rising stage of the curve for group A was steeper, and the rising stage of groups B, C, and D generally had a lower slope. Compared with groups B and C, the buffer platform period of group D was more obvious, and the peak stress reduction rate was smaller.

It can be seen from the above analysis that with the increase in freeze–thaw cycles in the same group of specimens, the more significant the damage inside the concrete makes it more prone to damage after impact, so the peak stress gradually decreases. In groups B, C, and D, due to the small bonding force between rubber and other aggregates, the incorporation of rubber introduces more gas, increasing the internal pores of concrete, and the hardness of rubber is less than that of other aggregates in concrete. These reasons make the specimen more prone to damage after impact, so the peak stress is smaller than that of group A. However, due to the large elasticity of rubber and the effect of absorbing energy, the concrete plays a buffering role after being impacted and absorbs part of the impact energy, which makes the concrete crushing process slow, the integrity improved, and the toughness better. The incorporation of rubber increases the internal pores of concrete and

increases the frost resistance of concrete, so that the peak stress of rubber concrete after freeze–thaw cycles decreases less after impact, which also confirms that the addition of an air-entraining agent to concrete can enhance the frost resistance of concrete [34]. In this experiment, it can be concluded that the frost resistance of group D is better.

3.4. Analysis of the Relationship between Dynamic Peak Stress and Strain Rate

Figure 6 shows the relationship between strain rate and peak stress of four groups of specimens (A, B, C, and D) under different freeze–thaw cycles and different impact strengths.

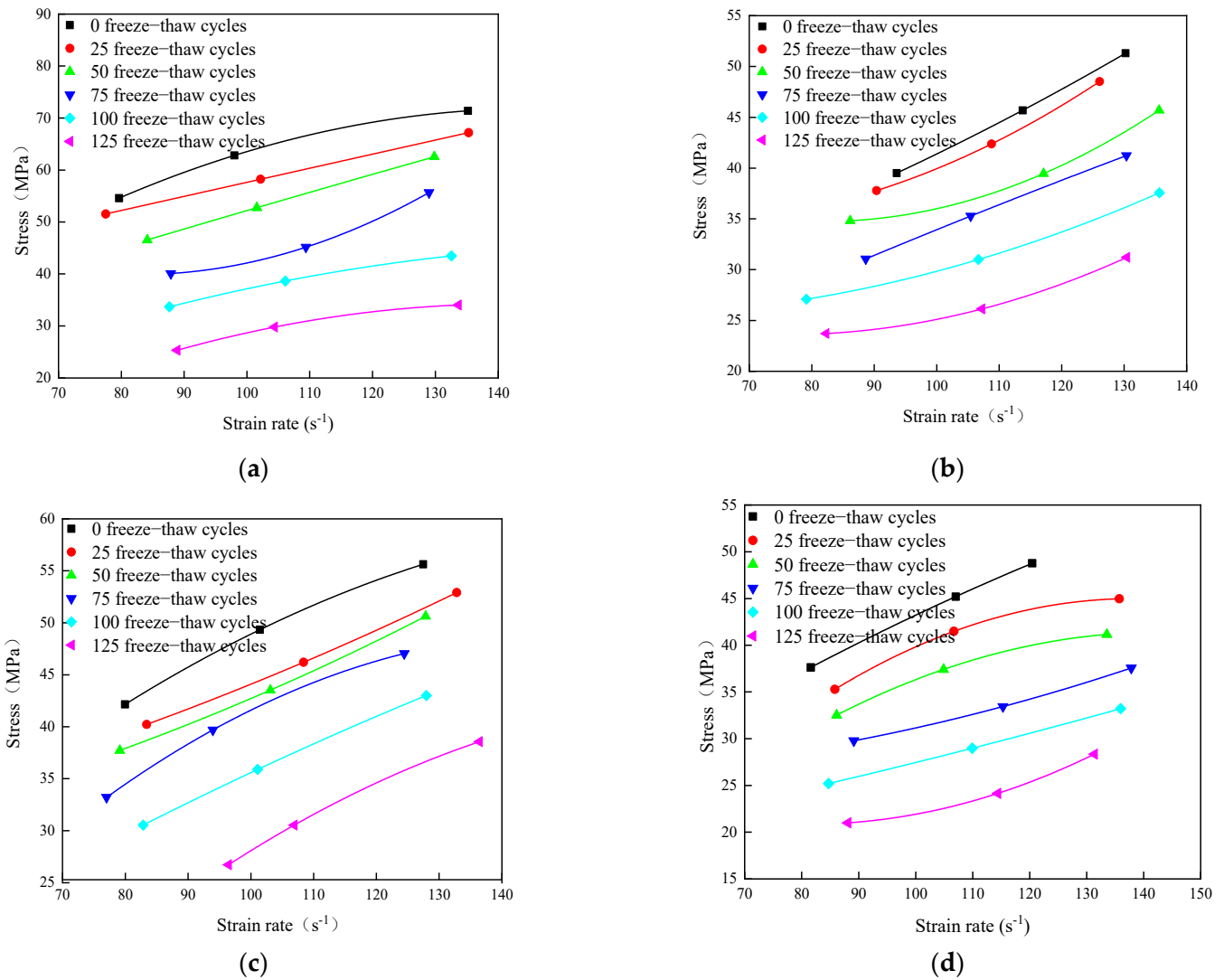


Figure 6. The relationship between strain rate and peak stress of each group. (a) The relationship between strain rate and peak stress of group A specimens. (b) The relationship between strain rate and peak stress of group B specimens. (c) The relationship between strain rate and peak stress of group C specimens. (d) The relationship between strain rate and peak stress of group D specimens.

From the above diagram, it can be seen that after the impact of the specimen in each group, as the strain rate increases, the dynamic peak stress of the specimen also increases. There is a certain positive correlation between the strain rate and the stress, which has a strong regularity. At the same time, the strain rate and the impact pressure also show a certain positive correlation. In the process of increasing the impact pressure, the strain rate enhancement effect of group A is similar to that of groups B, C and D, and there is no significant difference. It can be analyzed from the theory proposed by relevant scholars and the experimental phenomenon that this is because the specimen is subjected to rapid force

when it is impacted, the damage does not easily occur at the weakest point, and the energy propagates longer in the specimen. Therefore, when the impact pressure is larger, the failure time of the specimen is longer, and the strain rate is larger. The failure does not occur at the weakest point, and the energy propagation is more extensive in the specimen, which makes the failure force larger. Therefore, there is a certain positive correlation between impact pressure, strain rate, and dynamic peak stress.

3.5. Analysis of the Relationship between Dynamic Peak Stress and the Number of Freeze–Thaw Cycles

In order to explore the influence of rubber particle size on the dynamic peak stress during the freeze–thaw cycle, according to Table 4, the peak stress changes of groups A, B, C, and D after the freeze–thaw cycle under the same impact pressure were drawn. The specific line chart is shown in Figure 7.

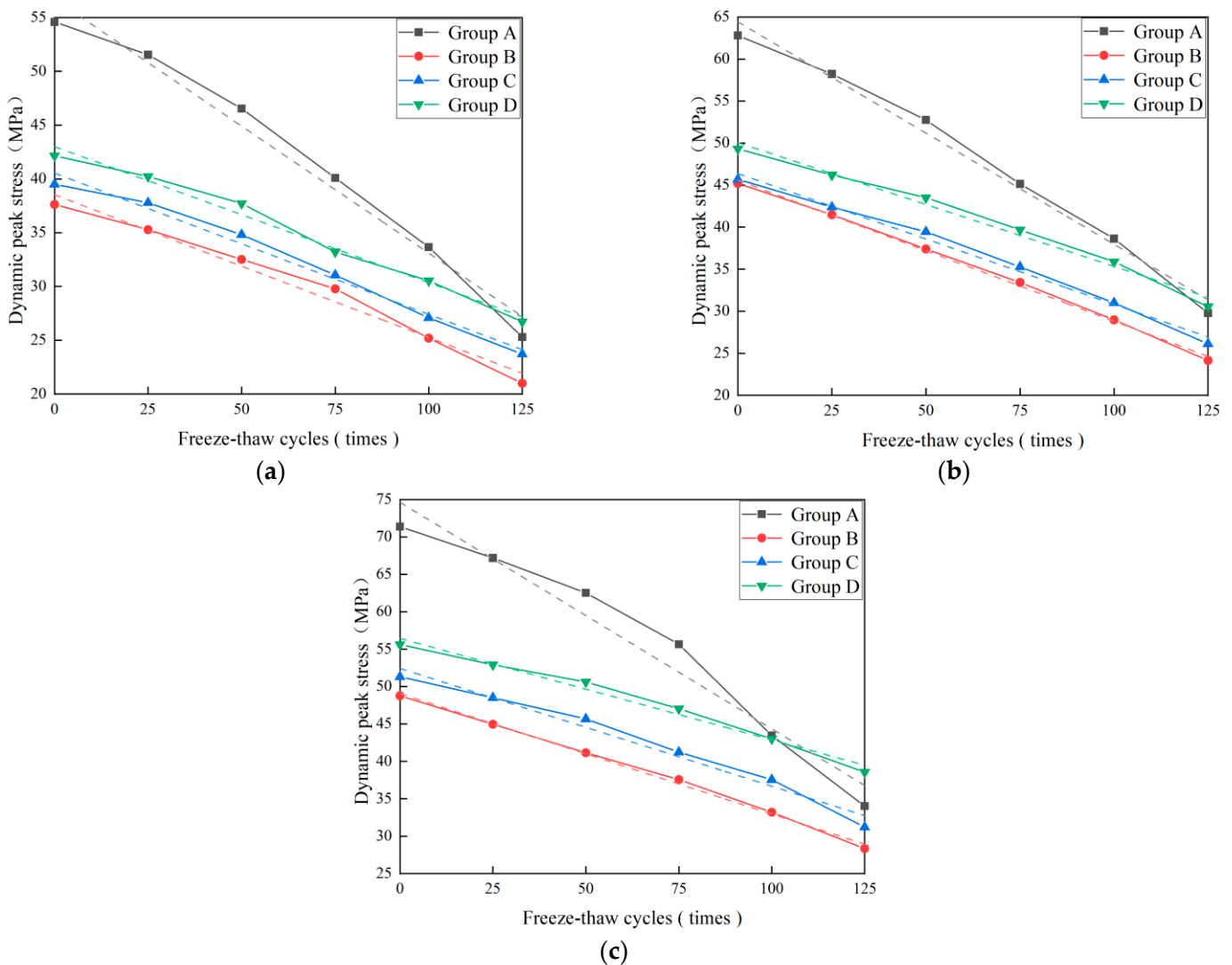


Figure 7. The relationship between the peak stress and the number of freeze–thaw cycles under different impact pressures. (a) The relationship between the number of freeze–thaw cycles and the peak stress of each group under 0.3 MPa. (b) The relationship between the number of freeze–thaw cycles and the peak stress of each group under 0.45 MPa. (c) The relationship between the number of freeze–thaw cycles and the peak stress of each group under 0.6 MPa.

It can be seen from Figure 7 that under the impact of three kinds of air pressure, the initial dynamic peak stress of group A is significantly larger than that of groups B, C, and D. With the increase in freeze–thaw cycles, the peak stress of the specimens

decreases continuously, and the dynamic peak stress of group A decreases significantly. The amplitude is greater than that of groups B, C, and D. After 125 freeze–thaw cycles, the dynamic peak stress of group A is even lower than that of group D, indicating that the addition of rubber can significantly improve the frost resistance of concrete. According to the slope of the dynamic peak stress of groups B, C, and D with the number of freeze–thaw cycles, it can be seen that the slope of group D is smaller than that of groups B and C. The peak stress of group A decreased by 53.6%, the peak stress of group B decreased by 44.2%, the peak stress of group C decreased by 40.0%, and the peak stress of group D decreased by 36.6%. At 0.45 Mpa pressure, the peak stress of group A decreased by 52.6%, the peak stress of group B decreased by 46.6%, the peak stress of group C decreased by 42.3%, and the peak stress of group D decreased by 38.1%. Under the impact of 0.6Mpa air pressure, the peak stress of group A decreased by 52.3%, the peak stress of group B decreased by 41.9%, the peak stress of group C decreased by 39.2%, and the peak stress of group D decreased by 30.7%. Therefore, the dynamic peak stress of group D decreased less with the increase in freeze–thaw cycles, indicating that the concrete mixed with 30-mesh rubber had the best frost resistance in this experiment. When the number of freeze–thaw cycles was 0, the dynamic peak strain of group D was higher than that of groups B and C, indicating that the addition of 30-mesh rubber in this experiment has the least effect on the peak compressive strength of concrete. In summary, the above analysis shows that the incorporation of rubber in concrete can significantly improve its frost resistance, and the incorporation of 30-mesh rubber has the best effect on improving the performance of concrete.

3.6. Analysis of the Relationship between Dynamic Peak Stress and Rubber Particle Size under Different Freeze–Thaw Cycles and Impact Pressure

The line chart in Figure 8 shows the relationship between dynamic peak stress of rubberized concrete with rubber particle sizes of 10 mesh, 20 mesh, and 30 mesh under different impact pressures. It can be concluded that under the same number of freeze–thaw cycles, as the diameter of the rubber particles increases, the dynamic peak stress of rubberized concrete gradually decreases, with the best performance observed for rubber particles of 30 mesh. Under the same number of freeze–thaw cycles, when the rubber particle sizes in the specimens are the same, the dynamic peak stress of the rubberized concrete gradually increases with higher impact pressures. With an increasing number of freeze–thaw cycles, the dynamic peak stress of the specimens after impact gradually decreases.

Based on the above relationships, it can be inferred that when the rubber particle size is smaller, it can better fill the gaps in the concrete, resulting in better particle distribution of various materials and a more compact and stable concrete structure. Additionally, a smaller rubber particle size leads to a smaller rubber particle surface area and less contact area between the rubber particles and aggregates. Since rubber, as an organic material, has weaker bonding with the various inorganic materials in concrete, a smaller contact area results in a smaller unstable bonding area, which increases the overall strength. In comparison to the impact process, in static compression testing, the loading rate of force is slower. During the loading process, there is sufficient time for the force to cause damage to the weakest part of the specimen. However, in dynamic impact testing, sudden loading leads to damage occurring throughout the specimen, making the testing more difficult and time-consuming. Therefore, the compressive strength in static compression testing is lower compared to that in dynamic impact testing. Similarly, among specimens from the same group with the same number of freeze–thaw cycles, the dynamic compressive strength is highest when the impact pressure is 0.6 MPa, followed by 0.45 MPa, and lowest with 0.3 MPa impact pressure.

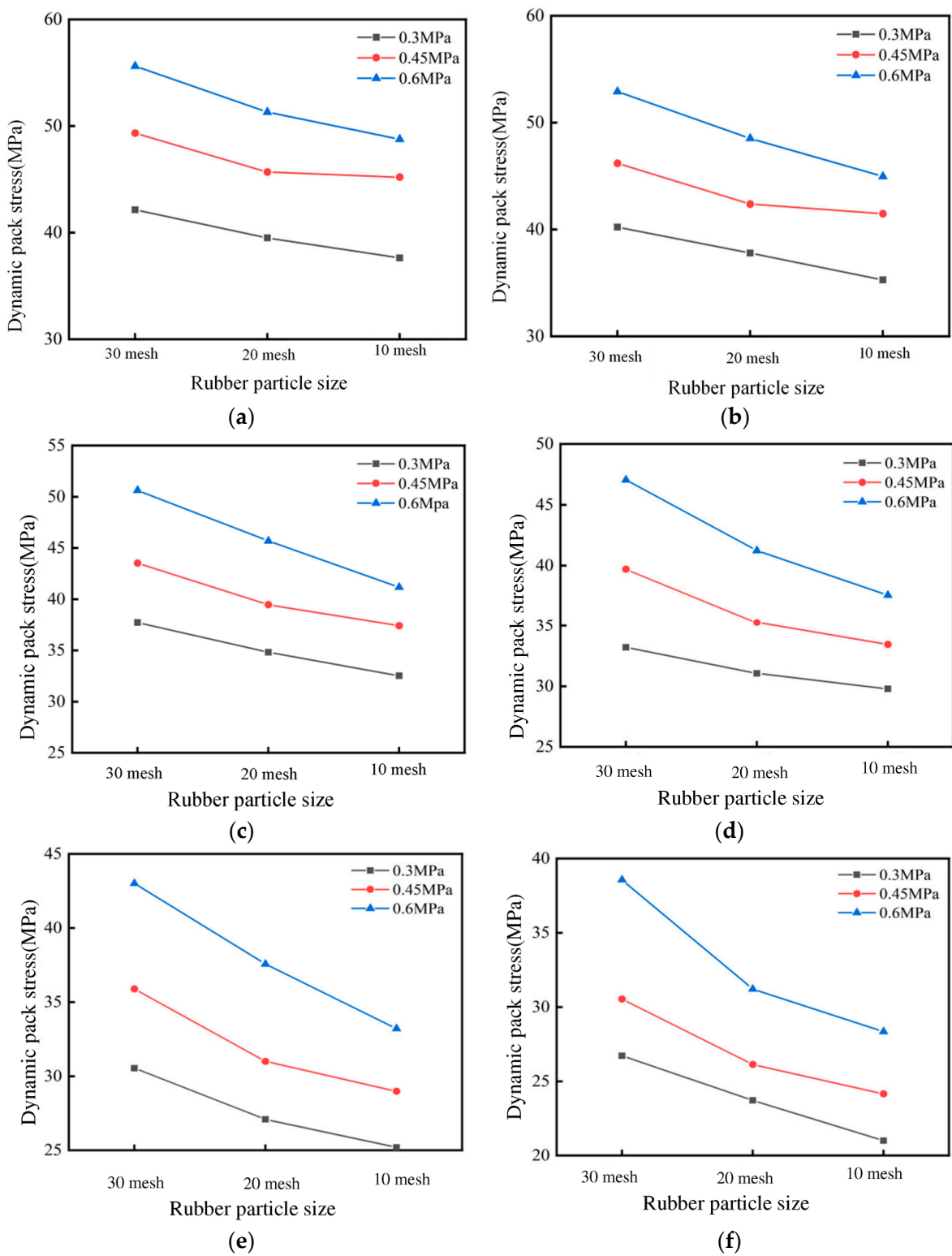


Figure 8. Relationship between peak stress and rubber particle size under different impact pressures after freeze–thaw cycles. (a) Rubber particle size peak stress relationship after 0 freeze–thaw cycles. (b) Rubber particle size–peak stress relationship after 25 freeze–thaw cycles. (c) Rubber particle size–peak stress relationship after 50 freeze–thaw cycles. (d) Rubber particle size–peak stress relationship after 75 freeze–thaw cycles. (e) Rubber particle size–peak stress relationship after 100 freeze–thaw cycles. (f) Rubber particle size–peak stress relationship after 150 freeze–thaw cycles.

4. Conclusions

In this study, freeze–thaw and impact tests were conducted on rubber concrete with different particle sizes to understand the impact mechanical performance of concrete materials under the influence of rubber particle size and freeze–thaw cycles and to reveal the mechanism of the effects of freeze–thaw cycles and rubber particle size on concrete material properties. Based on the above experimental results, the following conclusions can be drawn:

- (1) Under impact load, the concrete specimens show the coexistence of tensile failure and crushing failure mode, and the increase in impact pressure makes the fracture degree of the specimens increase. Under the same impact pressure, the crushing degree of ordinary concrete specimens is higher than that of rubber concrete specimens. After freeze–thaw cycles, rubber concrete still maintains a certain degree of integrity under high-pressure impact. The small pieces of debris on the edge of the specimen are peeled off, and the overall state is loose and not scattered. The incorporation of rubber particles can effectively improve the frost resistance and impact resistance of concrete.
- (2) Under impact load, as the strain rate increases, the dynamic peak stress of the specimen increases. There is a positive correlation between the strain rate and the dynamic peak stress, and there is also a positive correlation between the strain rate and the impact pressure. Under impact load, the peak stress of the 30-mesh rubber concrete specimen decreased the least after freeze–thaw cycles, and the peak stress was higher than that of the 10-mesh and 20-mesh rubber concrete specimens. Therefore, the incorporation of 30-mesh rubber in this experiment had the best effect on the frost resistance and impact resistance of concrete.
- (3) From the SEM analysis results, it can be seen that the incorporation of rubber particles makes the concrete denser, the number of large holes decreases, and more small pores are introduced. These pores alleviate the water pressure during the freeze–thaw process of concrete and the volume increases occurring during water freezing, and the degree of internal damage after freeze–thaw is relatively small. At the same time, rubber has a certain elasticity, which can effectively improve the impact resistance and integrity of concrete.

Author Contributions: X.H. wrote the manuscript; T.Y. edited the manuscript; J.Z. (Jinsong Zhang) designed research methods; J.Z. (Jun Zhang) edited and revised the manuscript; J.Z. (Jinsong Zhang) and T.Y., funding acquisition. All authors have read and agreed to the published version of the manuscript.

Funding: Supported by Open Research Fund of Anhui Province Key Laboratory of Green Building and Assembly Construction, Anhui Institute of Building Research & Design, Grant No. 2022-JKYL-007; Funded by the Natural Science Research Project of Higher Education Institutions in Anhui Province (2023AH051219); Funded by the Open Research Fund of The State Key Laboratory for Fine Exploration and Intelligent Development of Coal Resources, CUMT (SKLCRSM23KF00); Key Laboratory of Mine Construction Engineering in Anhui Province: Project Number: GXZDSYS2022102; Key Laboratory of Building Structures and Underground Engineering in Anhui Province: Project Number: KLBSUE-2021-01.

Data Availability Statement: Data are contained within the article.

Acknowledgments: The authors would like to thank the Editor-in-Chief, Editor, and anonymous reviewers for their valuable reviews.

Conflicts of Interest: The authors declare no conflicts of interest.

References

1. Karacasua, M.; Er, A.; Okur, V. Energy Efficiency of Rubberized Asphalt Concrete Under Low-temperature Conditions. *Procedia—Soc. Behav. Sci.* **2012**, *54*, 1242–1249. [[CrossRef](#)]
2. Kardos, A.J.; Durham, S.A. Strength, durability, and environmental properties of concrete utilizing recycled tire particles for pavement applications. *Constr. Build. Mater.* **2015**, *98*, 832–845. [[CrossRef](#)]

3. Turatsinze, A.; Measson, M.; Faure, J.-P. Rubberised concrete: From laboratory findings to field experiment validation. *Int. J. Pavement Eng.* **2018**, *19*, 883–892. [[CrossRef](#)]
4. Li, W.; Huang, Z.; Wang, X.C.; Zhang, J.P. Study on the Basic Performance and Noise Characteristics of Rubber Cement Concrete of Modified Latex. *Adv. Mater. Res.* **2014**, *953–954*, 1524–1527. [[CrossRef](#)]
5. Al-Tayeb, M.M.; Abu Bakar, B.; Ismail, H.; Akil, H.M. Effect of partial replacement of sand by recycled fine crumb rubber on the performance of hybrid rubberized-normal concrete under impact load: Experiment and simulation. *J. Clean. Prod.* **2013**, *59*, 284–289. [[CrossRef](#)]
6. Meng, L.; Li, C. Dynamic mechanical behaviour of recycled crumb rubber concrete materials subjected to repeated impact. *Mater. Res. Innov.* **2015**, *19* (Suppl. S8), S8-496–S8-501.
7. Zhu, Q.; Dai, H.; Chen, D.; Liang, Z. Study on Influence of Waste Tire Rubber Particles on Concrete Crack Resistance at Early Age. *IOP Conf. Series Earth Environ. Sci.* **2019**, *242*, 052060. [[CrossRef](#)]
8. Gholampour, A.; Ozbakkaloglu, T.; Hassanli, R. Use of Fine Rubber Particles as Fine Concrete Aggregates in Actively Confined Concrete. *Key Eng. Mater.* **2017**, *729*, 122–127. [[CrossRef](#)]
9. Bensaci, H.; Menadi, B.; Kenai, S.; Yahiaoui, W. Performance of self-compacting rubberized concrete. *MATEC Web Conf.* **2018**, *149*, 01070.
10. Huang, X.; Pang, J.; Liu, G.; Chen, Y. The influence of equal amplitude high stress repeated loading on the mechanical and deformation characteristics of rubber concrete. *Constr. Build. Mater.* **2021**, *266*, 121135. [[CrossRef](#)]
11. Thomas, B.S.; Gupta, R.C.; Mehra, P.; Kumar, S. Performance of high strength rubberized concrete in aggressive environment. *Constr. Build. Mater.* **2015**, *83*, 320–326. [[CrossRef](#)]
12. Zhu, H.; Liang, J.; Xu, J.; Bo, M.; Li, J.; Tang, B. Research on anti-chloride ion penetration property of crumb rubber concrete at different ambient temperatures. *Constr. Build. Mater.* **2018**, *189*, 42–53. [[CrossRef](#)]
13. Gupta, T.; Siddique, S.; Sharma, R.K.; Chaudhary, S. Behaviour of waste rubber powder and hybrid rubber concrete in aggressive environment. *Constr. Build. Mater.* **2019**, *217*, 283–291. [[CrossRef](#)]
14. Grinys, A.; Augonis, A.; Daukšys, M.; Pupeikis, D. Mechanical properties and durability of rubberized and SBR latex modified rubberized concrete. *Constr. Build. Mater.* **2020**, *248*, 118584. [[CrossRef](#)]
15. Rahul, K.; Manvendra, V.; Nirendra, D.; Nitin, L. Influence of chloride and sulfate solution on the long-term durability of modified rubberized concrete. *J. Appl. Polym. Sci.* **2022**, *139*, e52880.
16. Bengar, H.A.; Shahmansouri, A.A.; Sabet, N.A.Z.; Kabirifar, K.; Tam, V.W. Impact of elevated temperatures on the structural performance of recycled rubber concrete: Experimental and mathematical modeling. *Constr. Build. Mater.* **2020**, *255*, 119374. [[CrossRef](#)]
17. Pham, T.M.; Renaud, N.; Pang, V.; Shi, F.; Hao, H.; Chen, W. Effect of rubber aggregate size on static and dynamic compressive properties of rubberized concrete. *Struct. Concr.* **2021**, *23*, 2510–2522. [[CrossRef](#)]
18. Feng, W.; Liu, F.; Yang, F.; Jing, L.; Li, L.; Li, H.; Chen, L. Compressive behaviour and fragment size distribution model for failure mode prediction of rubber concrete under impact loads. *Constr. Build. Mater.* **2020**, *273*, 121767. [[CrossRef](#)]
19. Kadhim, A.A.; Al-Mutairee, H.M.K. An Experimental Study on Behavior of Sustainable Rubberized Concrete Mixes. *Civ. Eng. J.* **2020**, *6*, 1273–1285. [[CrossRef](#)]
20. Safeer, A.; Ayesha, F.; Saleem, K.S.M.; Junaid, M.M.; Shahid, A.; Ali, R.M. Effect of Particle Sizes and Dosages of Rubber Waste on the Mechanical Properties of Rubberized Concrete Composite. *Appl. Sci.* **2022**, *12*, 8460.
21. Zhang, J.; Zhang, G.; Sun, X.; Pan, W.; Huang, P.; Li, Z.; Zhang, B.; Zhou, X. An Experimental Study on the Compressive Dynamic Performance of Rubber Concrete under Freeze-Thaw Cycles. *Adv. Civ. Eng.* **2021**, *2021*, 6655799. [[CrossRef](#)]
22. Sukontasukkul, P. Use of crumb rubber to improve thermal and sound properties of pre-cast concrete panel. *Constr. Build. Mater.* **2008**, *23*, 1084–1092. [[CrossRef](#)]
23. Zhang, B.; Poon, C.S. Sound insulation properties of rubberized lightweight aggregate concrete. *J. Clean. Prod.* **2018**, *172*, 3176–3185. [[CrossRef](#)]
24. Azmi, A.A.; Abdullah, M.M.A.B.; Ghazali, C.M.R.; Sandu, A.V.; Hussin, K. A Review—Manufacturing on Rubberized Concrete Filled Recycled Tire Rubber. *Key Eng. Mater.* **2015**, *660*, 249–253. [[CrossRef](#)]
25. Thomas, B.S.; Gupta, R.C. A comprehensive review on the applications of waste tire rubber in cement concrete. *Renew. Sustain. Energy Rev.* **2016**, *54*, 1323–1333. [[CrossRef](#)]
26. Sulagno, B.; Aritra, M.; Jessy, R. Studies on Mechanical Properties of Tyre Rubber Concret. *Int. J. Civ. Eng.* **2016**, *3*, 18–21.
27. Yang, G.; Chen, X.; Xuan, W.; Chen, Y. Dynamic compressive and splitting tensile properties of concrete containing recycled tyre rubber under high strain rates. *Sadhana* **2018**, *43*, 178. [[CrossRef](#)]
28. Luo, D.; Xie, Y.; Su, X.; Wang, H.; Zhou, Y. Failure analysis of the damaged rubber concrete under the secondary load. *Strength Fract. Complex.* **2019**, *12*, 163–169. [[CrossRef](#)]
29. GB/T 50081; Standard for Test Method of Mechanical Properties on Ordinary Concrete. Beijing Standards Press of China: Beijing, China, 2016.
30. Li, L.; Qin, D.; Xu, Z.; Feng, Y. Study on Strengthening Mechanism of Epoxy Resin/Rubber Concrete Interface by Molecular Dynamics Simulation. *Adv. Civ. Eng.* **2022**, *2022*, 5100758. [[CrossRef](#)]
31. Shan, R.; Song, Y.; Song, L.; Bai, Y. Dynamic property tests of frozen red sandstone using a split hopkinson pressure bar. *Earthq. Eng. Eng. Vib.* **2019**, *18*, 511–519.

32. Gonen, T. Freezing-thawing and impact resistance of concretes containing waste crumb rubbers. *Constr. Build. Mater.* **2018**, *177*, 436–442. [[CrossRef](#)]
33. Ismail, K.M.; Hassan, A.A. Abrasion and impact resistance of concrete before and after exposure to freezing and thawing cycles. *Constr. Build. Mater.* **2019**, *215*, 849–861. [[CrossRef](#)]
34. Huang, C.; Chen, Y.; Wang, J.; Wang, Z.; Zhao, Q.; Zhu, L.; Wei, W.; Gao, Z. Study on dynamic compressive mechanical properties of freeze-thaw concrete. *Constr. Build. Mater.* **2022**, *322*, 126499. [[CrossRef](#)]

Disclaimer/Publisher’s Note: The statements, opinions and data contained in all publications are solely those of the individual author(s) and contributor(s) and not of MDPI and/or the editor(s). MDPI and/or the editor(s) disclaim responsibility for any injury to people or property resulting from any ideas, methods, instructions or products referred to in the content.